INSTITUTE OF PHYSICS PUBLISHING PLASMA SOURCES SCIENCE AND TECHNOLOGY
Plasma Sources Sci. Technol. **15** (2006) 64–71 doi:10.1088/0963-0252/15/1/010

Basic mechanisms controlling the sweeping efficiency of propagating current sheets

J W Berkery[1] **and E Y Choueiri**

Electric Propulsion and Plasma Dynamics Laboratory (EPPDyL), Mechanical and Aerospace Engineering Department, Princeton University, Princeton, New Jersey 08544, USA

E-mail: choueiri@princeton.edu and jwb2112@columbia.edu

Received 27 June 2005, in final form 19 October 2005
Published 16 December 2005
Online at stacks.iop.org/PSST/15/64

Abstract
The basic mechanisms controlling the sweeping efficiency of propagating current sheets are investigated through experiments and analytical modelling. The sweeping efficiency of a current sheet in a parallel plate gas-fed pulsed plasma accelerator is defined as the ratio of the current sheet mass to the total available propellant mass. Permeability of neutrals through the sheet, and leakage of mass out of the sheet and into a cathode wake, decrease the sweeping efficiency. The sweeping efficiency of current sheets in argon, neon, helium and hydrogen propellants at different initial pressures was determined through measurements of sheet velocity with high speed photography and of sheet mass with laser interferometry. The mechanism that controls the sweeping efficiency of propagating current sheets was found to be an interplay of two processes: the flux of mass entering the sheet and the leakage of mass at the cathode, with the former dependent on the degree of permeability and the latter dependent on the level of ion current as determined by the ion Hall parameter.

1. Introduction

A pulsed plasma thruster (PPT) is a type of electric space propulsion device that, in its pure electromagnetic version, uses a sheet of current and its interaction with a magnetic field to accelerate propellant gas to a high velocity. The present work investigates a specific inefficiency of electromagnetic PPTs that use gaseous propellants. PPTs can provide small impulse bits at high specific impulse, making them candidates for satellite attitude control or constellation positioning. Since higher efficiency of operation translates directly into reduced mass and cost of propellant, it is important to identify and quantify phenomena of the discharge that affect the performance of the device. Two major non-idealities of current sheet behaviour have been identified: current sheet canting [1, 2] and current sheet mass leakage. The tendency of mass to leak from the current sheet into a wake is explored in the present study.

Previous research has shown that the operation of these devices is not likely to follow the ideal pattern of the snowplow model. Recently, a study showed that the behaviour of current sheets was more complicated [1]. The study focused on the tendency of the current sheet to cant, or tilt, with the anode attachment leading the cathode attachment. This behaviour was evident under all conditions tested and is shown in figure 1. Also evident from the study and in figure 1 was that the current sheet seemed to be leaking plasma along the cathode as it travelled [2]. Although researchers have seen current sheet leakage in the past [1–10], and several researchers have noted the potential for a canted sheet to direct ions towards the cathode [1–5], a study of mass leakage as a function of propellant species has never been performed. Also, knowledge of the fundamental physics behind the leakage phenomenon and its effect on the sweeping efficiency of the current sheets was lacking.

The goal of the present study is to uncover the basic mechanism of current sheet mass leakage and to determine its effect on the sweeping efficiency of current sheets in gas-fed pulsed plasma accelerators. This is accomplished by making

[1] Present address: Postdoctoral Research Scientist, Department of Applied Physics and Applied Mathematics, Columbia University, New York 10027, USA.

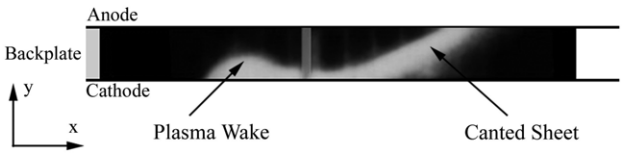

Figure 1. Photograph of a discharge from [11], showing two non-idealities of current sheet behaviour. The top electrode is the anode and the bottom electrode is the cathode. The plasma is moving from left to right. The ideal behaviour would be for the current sheet to be perpendicular to the electrodes. Instead we see a canted sheet and a plasma wake trailing the sheet along the cathode. The vertical bar in the middle of the photograph is a physical structure that obscured the light, not a plasma structure.

experimental measurements of the sweeping efficiencies of current sheets under different conditions of propellant pressure and species and then comparing these measurements to a model that explains the observed trends. We will show that two distinct modes of leakage exist and that these modes strongly affect the sweeping efficiency of the sheets.

We start with a description of the experimental apparatus and the diagnostics. We then report the experimental measurements leading to the measurement of the sweeping efficiency. First the measurements of current sheet velocity are presented. These measurements are then used together with time-resolved electron number density, in section 4.4, to determine the mass of the current sheet, which in turn gives the sweeping efficiency of the current sheet. A discussion of the experimental results is followed by a model that explains the observed trends of the sweeping efficiency. Finally we discuss the insight that is gained by using this model to explain the measurements.

2. Apparatus

The device used in this study has been previously described in detail [1]. Only a brief description will be provided here. The accelerator is not an actual thruster, but rather an idealized parallel plate accelerator with Pyrex sidewalls that allow good optical access to the discharge. The anode and cathode are made of copper and the area of the acceleration region measures 60 cm long and 10 cm wide, with a gap of 5 cm between the plates. The initial propellant distribution is a uniform gas fill. A pulse forming network is used to supply a current pulse with an approximately constant current of ~60 kA for 25 μs. Figure 2 shows a schematic and photographs of the accelerator.

3. Diagnostics

Likewise, the specific diagnostics used in this study have also been described in detail [1, 12]. These include a high-speed camera and a laser interferometer. The camera used was a Hadland Photonics Imacon 792LC camera with a framing rate of 500 000 frames per second. The camera was used to photograph the current sheets, through the Pyrex sidewalls of the accelerator, as they travelled down the electrodes. These photographs were used to measure the velocity of the current sheets under various conditions. The laser interferometer was used to make time-resolved measurements of the electron number density in the current sheet. With certain assumptions,

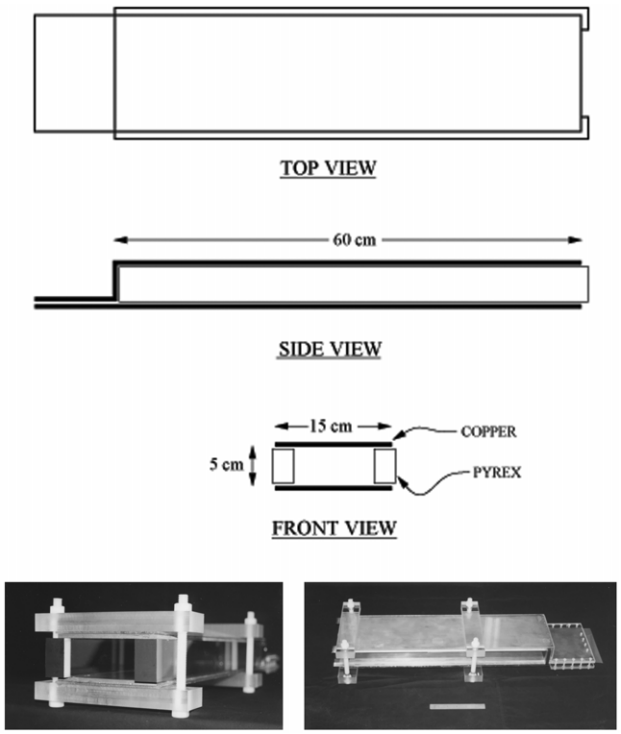

Figure 2. Schematic and photographs of the parallel plate accelerator.

the density and velocity of the sheet can be used together to estimate the current sheet mass.

4. Experimental results

York and Jahn [7] introduced a 'sweeping parameter' which is the percentage of available mass contained in the sheet. This parameter, which is essentially a measure of the sweeping efficiency of the sheet, is defined as

$$\Phi_{\mathrm{sh}} = \frac{m_{\mathrm{sh}}}{m_{\mathrm{av}}}, \tag{1}$$

where m_{sh} is the mass of the sheet and m_{av} is the total available mass. In the experiments presented here, the accelerator is operated with a uniform gas fill, so the available mass is simply the density of the gas fill times the volume of the accelerator. The sweeping efficiency is a first-order indicator of the severity of the current sheet mass leakage problem. It does not address the percentage of the lost mass that is contained in the slow moving wake, nor does it address the contribution of that wake to the total impulse of the device. Nonetheless, it is a useful parameter to gauge the leakage and its dependence on propellant species and pressure.

Measuring the sweeping efficiency of current sheets under various conditions requires a measurement of the current sheet mass. In order to measure the mass of the sheet, the velocity and time-resolved electron number density were measured and used together to integrate the density across the width of the sheet. The propellants used were hydrogen, helium, neon and argon, each with a fill pressure of 75–400 mTorr. For all conditions, the capacitor bank was charged to 9 kV, for an input energy of 4050 J and a current of approximately

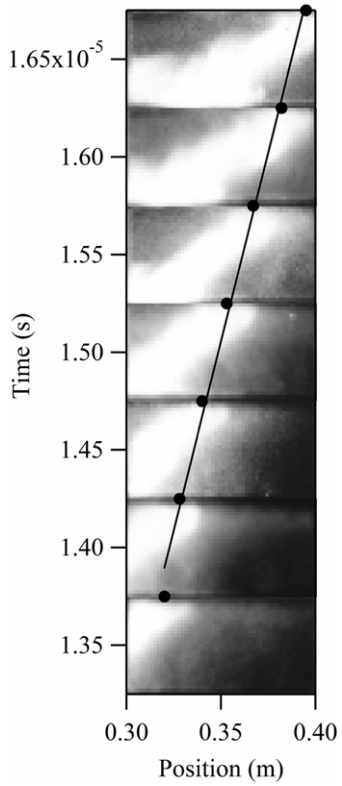

Figure 3. Time versus position for a series of photographs taken in an argon discharge at 100 mTorr. The images are interleaved from four separate discharges.

60 kA. The data are presented first from measurements of the current sheet velocity, second from measurements of electron number density and finally these two measurements are used to calculate the current sheet mass and sweeping efficiency.

4.1. Current sheet velocity measurements

The velocity of the current sheet is an important parameter for determining the performance of the accelerator, and it is required to calculate the current sheet mass, in subsection 4.4. The method employed to measure the current sheet velocity was high-speed photography. Using a camera that captured a frame every 2 μs, it is possible to track the distance versus time of the current sheet. A sample series of photographs is shown in figure 3. Note that several series of photographs from separate discharges were interleaved to obtain a time resolution greater than 2 μs. This is possible because the discharge is very repeatable. We also find that the velocity of the sheet asymptotes to a constant steady-state value after the first 10–20 cm of propagation [13]. Velocity measurements made with magnetic field probes also agree with the photographically measured velocity [13].

Figures 4 and 5 show the current sheet velocity measured for each propellant over a range of pressures. The error bars on the measured velocity data are standard deviations of the linear fits of position versus time, taking into account also an uncertainty on the position measurement of ± 1 cm. Typically four photographic series were interleaved to obtain between four and twelve position measurements per condition

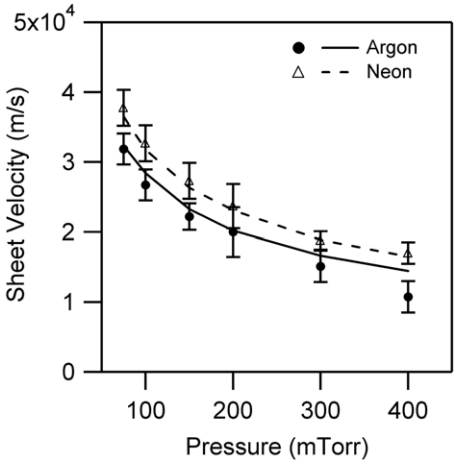

Figure 4. Current sheet velocity versus pressure for argon and neon. The velocity was measured with high speed photography and is compared with the expected value from a simple force balance (equation (3) with $X = 0.2$ for argon and $X = 0.3$ for neon).

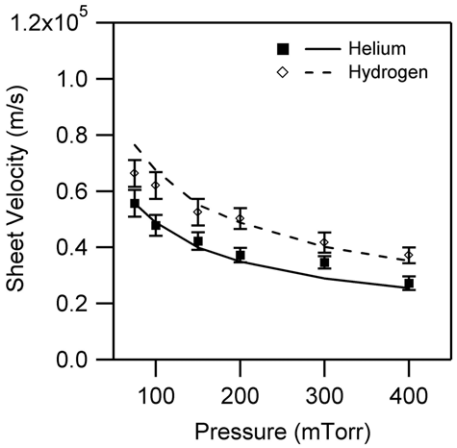

Figure 5. Current sheet velocity versus pressure for helium and hydrogen. The velocity was measured with high speed photography and is compared with the expected value from a simple force balance (equation (3) with $X = 1$ for helium and equation (4) with $X = 1$ for hydrogen).

(depending on the velocity of the sheet, it remained in the field of view of the camera for more or less frames).

4.2. Expected velocity of the sheet

The measurements of sheet velocity are compared, in figures 4 and 5, with the 'snowplow' velocity. The snowplow velocity is calculated from a balance between the force pushing the sheet and the opposing pressure drag of the ambient neutrals ahead of the sheet. Parallel to the electrodes (in the x direction), the force balance is

$$\frac{1}{2}L'J^2 = X\rho_a v_x^2 \frac{hd}{\cos^2\theta}, \tag{2}$$

where L' is the inductance per unit length of the device, J is the total current, θ is the canting angle, X is the fraction of neutral particles that is swept up by the sheet, h is the inter-electrode distance, d is the width of the electrodes, ρ_a is the ambient gas density, and $v_x = v\cos\theta$ is the snowplow

velocity in the x direction. The force on the left hand side of the equation comes from the $\boldsymbol{j} \times \boldsymbol{B}$ force and Ampere's law (the inductance per unit length is a geometric factor that also includes μ_0 [14]). The force on the right hand side of the equation is the x component of the pressure drag of the ambient neutral particles ahead of the sheet.

Solving for the snowplow velocity in the x direction, we find

$$v_x = \sqrt{\frac{(1/2)L'J^2\cos^2\theta}{X\rho_a hd}}. \tag{3}$$

The inductance per unit length of our device is based on the geometry and thus is constant at a value of 3.845×10^{-7} H m^{-1}. Likewise, the height and depth, h and d of the device were constant at 5.08 cm and 10.16 cm, respectively. Since all of the data reported here were taken with the same applied voltage, the total current J was very similar, though not exactly the same, in all the cases (typically ~60 kA). The current was measured with a current transformer, and the flat-top value of the current was used in equation (3). The initial gas fill density is straightforwardly calculated from the initial propellant pressure, measured with a Baratron gauge. The values of θ used in the calculations were obtained from the work of Markusic *et al* [1, 11] and from the present research. Measurements of θ from various methods have shown that θ increases with increasing atomic mass of the propellant. The specific values used for θ for this and subsequent calculations are argon: 60°, neon: 60°, helium: 50° and hydrogen: 16°.

The force balance performed here makes the approximation that the sheet acts as a solid body and transfers momentum perfectly to a certain fraction, X, of the stationary neutral atoms. This is the only term in equation (3) that is unknown. By measuring the current sheet velocity and comparing with the expected velocity from equation (3), however, we can determine the effective amount of 'permeability' of the sheet $(1 - X)$ that can explain the measurements. Since the parameter X is inferred from these velocity measurements, it will not represent a free parameter when used in the model of section 6.

Hydrogen is a special case, however, because the protons comprising the sheet have half the mass of the diatomic molecules they collide with. In this case, conservation of momentum and energy of the colliding particles show that for an elastic collision the final velocity of the diatomic molecule is two-thirds the incident velocity of the ion and the ion will recoil at one-third of its original velocity. Therefore, while protons in the sheet can be locally accelerated to the snowplow velocity, the velocity of the sheet is equal to the mean velocity of the ions and thus should be limited to two-thirds the snowplow velocity. We find that this is the case for hydrogen. In figure 5, the plotted theoretical velocity for hydrogen is

$$v_H = \frac{2}{3}\sqrt{\frac{(1/2)L'J^2\cos^2\theta}{X\rho_a hd}}. \tag{4}$$

We have also performed a limited amount of velocity measurements of current sheets in deuterium, and they have shown the same two-thirds limitation.

4.3. Current sheet electron number density measurements

With a few assumptions, electron density measurements in the current sheet will allow us to calculate the current sheet mass and therefore the sweeping efficiency. In this subsection we will present the electron number density measurements themselves. In the next subsection we use these measurements to determine the sheet mass.

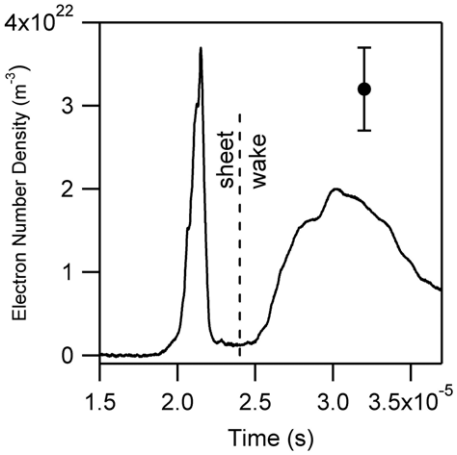

Figure 6. Measurement of electron number density versus time for argon: 300 mTorr, 9 kV. The first peak is the sheet and the second peak is the wake. A typical error bar (based mainly on the repeatability of the peak density measurements) is also shown.

The laser interferometer used in these studies provides an electron number density measurement at a single spatial location with time resolution. The data presented here are from measurements at a single location in the thruster for each propellant, corresponding to the laser interferometer beam positioned in the middle of the electrode gap, at 38 cm from the backplate for argon and 51.5 cm from the backplate (8.5 cm from the exit) for all other propellants. These measurements were made at these locations ten times at each propellant and pressure setting, from 75 to 400 mTorr.

An example of a single, time-resolved, electron number density measurement is shown in figure 6. In this particular case, the sheet and wake structures are very clearly visible. The first peak of density is the current sheet, while the second peak is the wake.

4.4. Calculation of the sweeping efficiency

The mass of the current sheet can be determined from the time-resolved electron density measurement. First, we will assume that the plasma in the sheet is singly ionized, therefore the electron number density is equal to the ion number density. Second, we will assume that the sheet is fully ionized, so that ions make up the entire mass of the sheet. Previous spectroscopic measurements have shown the current sheet electron temperature to be approximately 2.4 eV in argon [11] and 2.6 eV in neon [13]. At this temperature and the densities measured here, these assumptions are likely to be valid.

The mass of the current sheet, then, is the density integrated over the volume,

$$m_{sh} = \int \rho_i \, dV = \iiint m_i n_e \, dx \, dy \, dz. \tag{5}$$

In our experiment, the sheet is uniform in the z direction (out of the page in figure 1), therefore the dz term immediately comes out of the integral as d, the 'depth' of the electrodes.

In the y direction, the plasma density is not uniform. However, we have seen from a detailed map of the number density for argon at 100 mTorr that the increase in the electron number density from the anode to the cathode is very linear. Therefore measuring electron number density at the middle of the electrode gap and multiplying by the height of the sheet is equivalent to taking an average, and the $\mathrm{d}y$ term becomes simply h.

The electron number density has been measured at a given spatial location, with time resolution. This can easily be turned into a spatially resolved measurement in x across the sheet by multiplying by the velocity, which is known. Therefore the expression for the sheet mass becomes

$$m_{\mathrm{sh}} = m_{\mathrm{i}} h d \int n_{\mathrm{e}} v_{\mathrm{sh}} \, \mathrm{d}t. \tag{6}$$

Care must be taken, however, to integrate only across the sheet and not the wake. The integration must be cut off, then, at a time after the sheet has passed and before the wake has arrived. Figure 6 shows an example of an interferometry trace showing the separation point between the sheet and wake densities. The uncertainty associated with the connection of the two structures (the density does not always go to zero between them) is small compared with the integrated mass of the entire sheet ahead of that point.

The sheet mass was calculated in this way, using equation (6) with the electron number density measurements and the velocity measurements of section 4.1, for each propellant over the usual range of pressures (75–400 mTorr). For each propellant, at each pressure setting, ten interferometry measurements were made and used to calculate the current sheet mass. The standard deviation of the ten calculations is used to calculate the error in the sweeping efficiency measurements.

It should be noted, again, that the laser beam is positioned close to but not exactly at the exit of the accelerator, especially for the measurements in argon. However, we have seen that the canting angle, the velocity and the electron number density do not change significantly after an initial transient time during which the canted sheet is fully established. This time varies for the various conditions tested, but the steady-state propagation phase usually begins within the first 10–20 cm. Measurements of sheet velocity, canting angle and density in the steady-state phase are constant within the error bars of the measurements [13]. The mass and impulse at the exit plane should thus be very closely approximated by our measurements.

In equation (1) we defined the sweeping efficiency. Using the mass measurements from equation (6), we can now calculate the sweeping efficiency of the thruster over the range of conditions studied. Figures 7 and 8 show the sweeping efficiency versus pressure for argon and neon, and helium and hydrogen, respectively. Also included in these figures are the results of a model presented in section 6.

5. Discussion of experimental results

We have presented measurements of the current sheet velocity and sweeping efficiency for a range of initial propellant fill pressures of 75–400 mTorr for argon, neon, helium and hydrogen. These measurements provide insight into the phenomenon of current sheet mass leakage. Specifically, the sweeping efficiency provides a basis for determining the severity of the problem and its trends with pressure and propellant atomic mass.

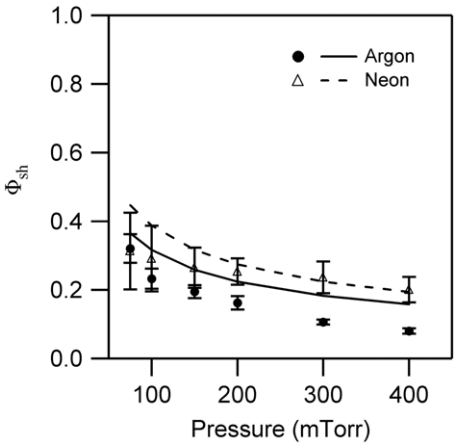

Figure 7. Φ_{sh} versus pressure, for argon and neon. The markers are experimental measurements from section 4.4, and the lines are predictions from the model, from section 6.

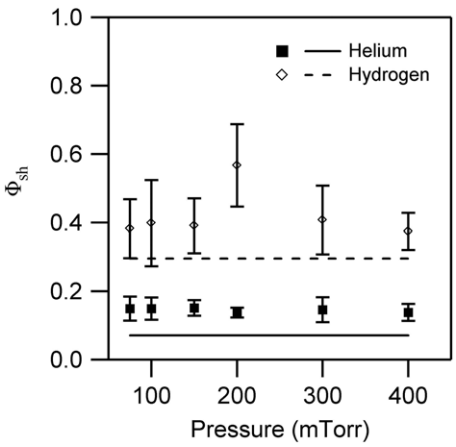

Figure 8. Same as figure 7, but for helium and hydrogen.

In figures 4 and 5, the velocities of current sheets measured with photography were plotted versus propellant fill pressure for each propellant. We can see that the snowplow velocity predicted from a force balance (equations (3) and (4)) correctly predicts the measured velocity for helium and hydrogen.

For argon and neon, however, the predicted velocity for impermeable ($X = 1$) sheets is significantly lower than the velocities that were measured. The high measured velocities can be explained only by a permeability of ~80% for argon and ~70% for neon. The implied permeability of these sheets is consistent with other data from our research and density measurements of the 'restrike' current sheet. When the current from the pulse forming network reverses (after 25 μs), a second current sheet is created that is of significant density in argon and neon discharges, but has almost zero density in helium and hydrogen discharges. This indicates that a significant amount of neutral propellant is left behind in the thruster chamber by

argon and neon discharges, but not by helium and hydrogen discharges.

Figures 7 and 8 show the sweeping efficiency, Φ_{sh}, versus pressure for each propellant. For the heavier propellants the efficiency decreases with increasing propellant fill pressure. In other words, for argon and neon the sheet mass does not increase at a rate commensurate with the increase in propellant pressure. For helium, the sweeping efficiency stays constant with pressure, but it is fairly low, around 20%. For hydrogen, Φ_{sh} is also constant with pressure at around 40%, with the exception of the 200 mTorr measurement. We believe that the random error on both the density and velocity measurements compounded in this case to cause the one measurement to appear high. We do not believe that this single point is indicative of a trend.

6. A model of the current sheet

We wish to explain and predict the experimentally determined sweeping efficiency trends both qualitatively and quantitatively. In order to do this, we must construct a model of the mass sweeping process. The main goal of the model is to gain insight into the important processes that cause the trends of the data that we observed. We have chosen to avoid the use of computer simulations in favour of an analytical approach which has the promise of giving more accessible, albeit less detailed, insight.

In order to simplify the analysis, let us consider a current sheet with a constant electron density and temperature everywhere across its width and height. In the steady-state condition that we observe, the sheet asymptotes to a constant velocity, canting angle and mass. In this case, the density of the sheet can be determined by balancing the fluxes of mass into and out of the sheet. A mass flux balance for the sheet is given by

$$\frac{\partial m_{sh}}{\partial t} = 0 = \Gamma^e - \Gamma^l. \tag{7}$$

Here, Γ^e is the flux of mass entering the sheet, and Γ^l is the flux of mass leaking from the sheet at the cathode and entering the wake.

The first term can be expressed as

$$\Gamma^e = X\rho_a v_x h d, \tag{8}$$

which is the percentage of the neutrals that is swept up, X, times the density of the neutrals, times the sheet velocity, times the frontal area of the sheet.

If we define the velocity of plasma out of the sheet and into the wake at the cathode to be v_c and the sheet width in the x direction to be w, the sheet loses mass at a rate

$$\Gamma^l = \rho_i v_c w d. \tag{9}$$

This means that, with $\Gamma^e = \Gamma^l$, we find

$$\frac{\rho_i}{\rho_a} = X\frac{h}{w}\frac{v_x}{v_c}. \tag{10}$$

Also the sweeping efficiency can be written as

$$\Phi_{sh} = \frac{\rho_i h d w}{\rho_a h d l}, \tag{11}$$

where l is the total length of the electrodes. Together with equation (10), this gives us

$$\Phi_{sh} = X\frac{h}{l}\frac{v_x}{v_c}. \tag{12}$$

We see that the sweeping efficiency depends on the permeability of the sheet, the geometry of the device and the axial velocity of the sheet compared with the velocity of plasma into the wake. In order to complete our model of the sweeping efficiency of the sheet, we must consider the cathode boundary condition, specifically the flux of plasma from the sheet into the wake.

6.1. The motion of ions in the current sheet

Let us consider a current sheet in the moving frame of reference. A neutral particle moves with velocity v_x towards the sheet and at some point in the sheet it is ionized. The newly created electron will immediately begin drifting in the crossed electric and magnetic fields. Lovberg pointed out that if the newly created ion is free to gyrate it will also begin a drift motion, and no polarization field between the two particles will arise [15]. However, if the ion's Hall parameter (Ω_i) is low, it will initially remain stationary as the electron moves away, creating a polarization field. This will serve to decelerate the ion (in the sheet frame of reference) to zero velocity.

The former case (high ion Hall parameter) was observed by Lovberg in hydrogen current sheets, as evidenced by a lack of measured polarization field and an implied high level of ion current [15]. The low ion Hall parameter case was observed in a heavier propellant, nitrogen, where polarization fields were measured and the ion current component was effectively zero [15]. This distinction in behaviour is important for us to consider because the leakage of mass out of the sheet depends on the velocity of ions towards the cathode, or the ion current. In our experiments the ion Hall parameter is calculated to be on the order of 1 for helium and hydrogen and less than 0.1 for argon and neon.

In the case where $\Omega_i \approx \mathcal{O}(1)$, the ions' motion is determined by their drift velocity. From the ion and electron momentum equations in steady-state and neglecting the pressure gradient terms, we find that,

$$\boldsymbol{u}_i = \frac{\Omega_i}{e n_e}\frac{\boldsymbol{j}\times\boldsymbol{B}}{B}. \tag{13}$$

The ions move perpendicularly to the current, and thus their cathode-directed velocity is related to the sheet velocity by $v_c = v_x \tan\theta$ (see figure 9).

Alternatively, in the limit of $\Omega_i \ll 1$, ions are not able to complete a drift motion, so their motion is determined entirely by the polarization field in the x direction. Electrons carry all of the current, and there is no directed leakage of ions at the cathode (see figure 10). Since the directed leakage has been reduced to effectively zero in this case, the dominant leakage process is instead diffusion. Therefore, for the flux of particles leaking out of the sheet we use

$$\Gamma^l = \rho_c\left(\frac{\bar{c}}{4}\right)wd = \rho_c w d\frac{1}{4}\left(\frac{8kT_e}{\pi m_i}\right)^{1/2}. \tag{14}$$

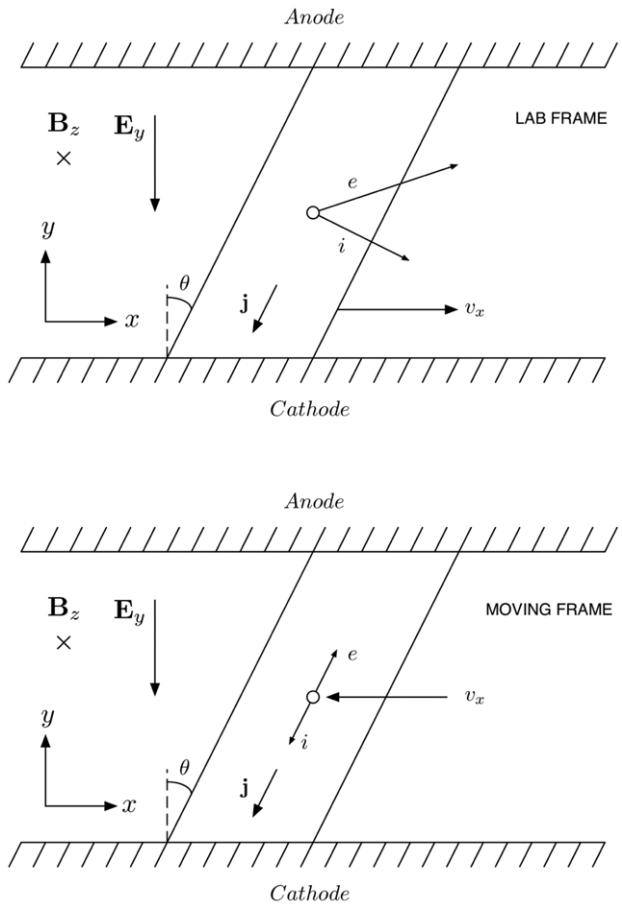

Figure 9. Diagram of the behaviour of ions and electrons in the lab frame and moving frame when $\Omega_i \sim 1$. Both ions and electrons are free to follow drift motions, and no polarization field arises. The resulting ion current constitutes a *directed* leakage of plasma.

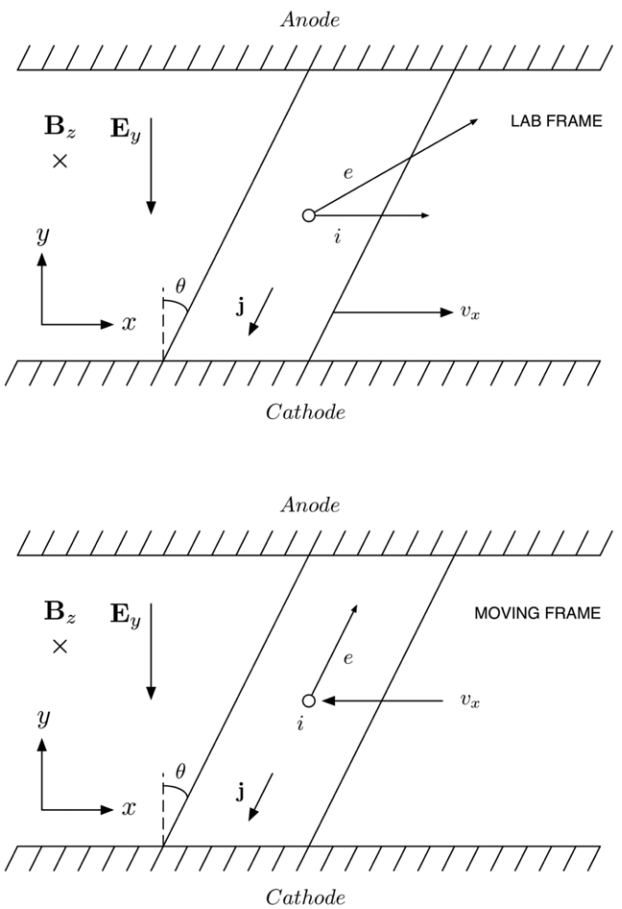

Figure 10. Diagram of the behaviour of ions and electrons in the lab frame and moving frame when $\Omega_i \ll 1$. The motion of ions is entirely due to the polarization electric field that arises from a charge separation of ions and electrons. In the moving frame this field is just sufficient to decelerate the ions to zero velocity in the sheet. With no ion current, the leakage of plasma at the cathode is *diffusive*.

Here we have deviated from our previous simplification of a constant ion density in the entire sheet by defining instead a density at the cathode ρ_c. This is because we have found experimentally that the density in the sheet increases from anode to cathode, such that the average density relates roughly to the cathode density by $\rho_i \approx (2/3)\rho_c$.

We have identified two limits of the current sheet mass leakage behaviour: the directed mass flux leakage which dominates when the ion Hall parameter is on the order of 1 and the diffusive mass flux leakage which dominates when $\Omega_i \ll 1$. In the first case we see that the expression for the sweeping efficiency reduces to

$$\Phi_{sh} \approx X \frac{h}{l} \frac{1}{\tan\theta}. \tag{15}$$

When diffusion is the dominant mode of mass leakage at the cathode, Φ_{sh} is calculated from the expression

$$\Phi_{sh} \approx X \frac{2}{3} \frac{h}{l} \frac{v_x}{(\bar{c}/4)}. \tag{16}$$

Sheet velocity measurements give us X and v_x, but the electron temperature must also be known to calculate $\bar{c}/4$. We have measured the electron temperature in neon current sheets spectroscopically and have found a temperature of about 2.6 eV for the whole range of pressures. This is close to Markusic's measurement of 2.4 eV in an argon, 100 mTorr discharge [11]. The value 2.6 eV will be used in all calculations.

6.2. *Results of the model*

Figures 7 and 8 show the measured sweeping efficiencies in argon and neon, and helium and hydrogen, respectively, with the modelled results included. We find that the diffusive leakage model captures the trend of the sweeping efficiency of argon and neon current sheets well, while the directed leakage model describes helium and hydrogen current sheets. Therefore, the modelled Φ_{sh} in figure 7 is the calculated value from equation (16), while the curves in figure 8 are calculated from equation (15).

For the most part, and considering the simplicity of the model, the model results match the experimental results well. Although the predictions from equation (15) are slightly low compared with the helium and hydrogen measurements, they capture the lack of dependence of the sweeping efficiency on pressure for these sheets. The argon and neon measurements, by contrast, show a dependence on propellant fill pressure,

which is captured by the model through equation (16). Here the model's predictions are slightly high. Qualitatively this is encouraging because diffusive leakage is the minimum expected flux. Any small amount of directed leakage that exists in these sheets will tend to lower the predicted sweeping efficiency, bringing the model results closer to the measurements. Having verified the model as a good predictor of the observed behaviour, we can now consider the insights that we have gained from it.

6.3. Insight gained from the model

The purpose of creating a simplified model of the current sheet is to gain insight about the various factors that influence the sweeping process. A computer model including all effects would perhaps give us a better prediction of measured quantities, but at the expense of complication that obscures insight. Our model tells us that the sweeping efficiency of a current sheet propagating into an ambient density of neutral gas is determined by the interplay of two processes: the flux of mass entering the sheet and the leakage of mass at the cathode into the wake.

Current sheets of the heavier propellants (argon and neon) are found to differ from the current sheets of the lighter propellants (helium and hydrogen) in behaviour in both of these processes. Comparison of the measured current sheet velocities to the predicted velocities show that the heavier propellant current sheets are subject to permeability, while the lighter propellants are not. Permeability reduces the flux of mass entering the sheet while increasing the sheet velocity. Comparison of the measured sweeping efficiencies to the predicted sweeping efficiencies show that the heavier propellant sheets are better described by a diffusive leakage model, while the lighter propellant sheets are well described by a directed leakage model.

This means that the lighter propellant's sheets are impermeable to the neutrals, so they effectively sweep up propellant gas, but at the same time these sheets are prone to directed leakage of ions at the cathode. By contrast, argon and neon sheets are prone to permeability (perhaps due to an inefficiency of the polarization field in accelerating ions) but tend not to direct ions towards the cathode. Thus we have found that these sheets have higher permeability, but lower leakage.

This picture of the sweeping process of these current sheets points to the following expected impact on the performance of the device as a thruster. Operation with the heavier propellants should leave more unaccelerated propellant behind in the chamber due to permeability, while operation with lighter propellants should direct more mass in the wake due to leakage while not leaving much mass behind in the chamber. We have observed both of these trends in our experiments.

7. Conclusions

A study of the effect of mass leakage on the sweeping efficiency of current sheets in a gas-fed pulsed plasma accelerator has been presented. The major findings of this study are as follows.

- The measured sweeping efficiencies of helium and hydrogen current sheets are independent of propellant pressure over the range tested. These propellants, due to their relatively high ion Hall parameters, experience directed leakage of mass into the wake but very little permeability.
- The measured sweeping efficiencies of argon and neon current sheets decrease with increasing propellant pressure. These propellants, with relatively low ion Hall parameters, undergo mostly diffusive leakage but are also prone to current sheet permeability.
- The basic mechanism that controls the sweeping efficiency of propagating current sheets is an interplay between two processes: the flux of mass entering the sheet and the leakage of mass at the cathode into the wake. The flux entering the sheet is dependent on the degree of permeability while the leakage is dependent on the level of ion current as determined by the ion Hall parameter.

Acknowledgments

The authors gratefully acknowledge the help of Dr Tom Markusic and Mr Bob Sorenson in this work. This work was supported by the Program in Plasma Science and Technology, Princeton Plasma Physics Laboratory.

References

[1] Markusic T E, Choueiri E Y and Berkery J W 2004 *Phys. Plasmas* **11** 4847–58
[2] Markusic T E, Berkery J W and Choueiri E Y 2005 *IEEE Trans. Plasma Sci.* **33** 528–9
[3] Lovberg R H 1964 *IEEE Trans. Nucl. Sci.* **11** 187–98
[4] Johansson R B 1964 *Phys. Fluids* **8** 866–71
[5] Burton R L and Jahn R G 1968 *Phys. Fluids* **11** 1231–7
[6] MacLelland J R, MacKenzie A S V and Irving J 1966 *Phys. Fluids* **9** 1613–5
[7] York T M and Jahn R G 1970 *Phys. Fluids* **13** 1303
[8] Pert G J 1970 *Phys. Fluids* **13** 2185–92
[9] Keck J C 1962 *Phys. Fluids* **5** 630–2
[10] Fishman F J and Petschek H 1962 *Phys. Fluids* **5** 632–3
[11] Markusic T E 2002 Current sheet canting in pulsed electromagnetic accelerators *PhD Thesis* Princeton University
[12] Markusic T E and Choueiri E Y 2001 *37th Joint Propulsion Conf. (Salt Lake City, UT, 8–11 July)*
[13] Berkery J W 2005 Current sheet mass leakage in a pulsed plasma accelerator *PhD Thesis* Princeton University
[14] Kohlberg I and Coburn W O 1995 *IEEE Trans. Magn.* **31** 628–33
[15] Lovberg R H 1963 *Proc. of the 6th Int. Conf. on Ionization Phenomena in Gases (Paris, 8–13 July 1963)* vol 4 p 235–9